Article

Understanding Ni(II) Mediated C(sp3)-H Activation: Tertiary Ureas as Model Substrates

Douglas Dawson Beattie, Anna C. Grunwald, Thibaut Perse, Laurel L. Schafer, and Jennifer A. Love

J. Am. Chem. Soc., **Just Accepted Manuscript** • DOI: 10.1021/jacs.8b07708 • Publication Date (Web): 06 Sep 2018

Understanding Ni(II) Mediated C(sp^3)-H Activation: Tertiary Ureas as Model Substrates

D. Dawson Beattie, Anna C. Grunwald, Thibaut Perse, Laurel L. Schafer,* and Jennifer A. Love*

‡Department of Chemistry, The University of British Columbia, 2036 Main Mall, Vancouver, British Columbia, Canada V6T 1Z1

Nickel ● C-H activation ● urea

ABSTRACT: We report a mechanistic study of C(sp^3)-H bond activation mediated by nickel. Cyclometalated Ni(II) ureate [(PEt_3)Ni(κ³-*C,N,N*-(CH_2)N(Cy)(CO)N((N)-quinolin-8-yl))] (**3a**) was synthesized and isolated from urea precursor (**2a**), (Me)(Cy)N(CO)N(H)(quinolin-8-yl), *via* C(sp^3)-H activation. We investigated the effects of solvents and base additives on the rate of C-H activation. Kinetic isotope effect experiments showed that C-H activation is rate determining. Through deuterium labelling and protonation studies, we also showed that C-H activation can be reversible. We extended this reaction to a range of ureas (**2b,c,e-n**) with primary and secondary C(sp^3)-H bonds, which activate readily to form analogous nickelated products (**3b,c,e-n**). Finally, we showed that carboxylate additives assist with both ligand dissociation and initial N-H bond activation, consistent with a concerted metalation deprotonation mechanism.

Introduction

The selective activation of carbon-hydrogen (C-H) bonds by transition metals has long been a major research goal in the fields of organometallic chemistry and catalysis. Such reactions would permit the construction of functionalized molecules without prior activation of the coupling partners, improving step economy and minimizing waste. Despite remarkable success in the coupling of unactivated aryl C(sp^2)-H bonds, the functionalization of unactivated C(sp^3)-H bonds remains difficult. The main challenges are the low polarity (and thus low reactivity) of these bonds, and the difficulty of distinguishing between different C-H bonds. A number of strategies have been devised to overcome the inherent low reactivity, including: activated metal complexes,[1–4] carefully selected base additives,[5,6] and photo-redox methods.[7–11] The challenge in selecting one C-H bond over another can be overcome by the use of directing groups,[12–14] and in some cases judicious ligand selection.[15,16]

Transition metal-mediated C-H bond cleavage can occur through multiple reaction mechanisms. Metals in low oxidation states can activate C-H bonds by traditional oxidative addition pathways,[2,3] while other metals cleave C-H bonds by radical pathways.[17,18] Still others undergo redox neutral reactions such as sigma bond metathesis,[19,20] concerted metalation deprotonation (CMD),[5,12,21–23] ambiphilic metal ligand activation (AMLA),[20,24] or ligand-to-ligand hydrogen transfer (LLHA).[25] Even for a single transition metal complex, several mechanisms may be accessible, which can lead to competing processes and thus lower selectivity and reaction yield. As such, it is imperative to develop a detailed mechanistic understanding of these elementary reactions.

CMD has been found to be common in catalytic C-H activation with group 10 metal complexes. In particular, the mechanism has been studied in depth for palladium(II) complexes.[21–23,26,27] Computational reports by several research groups point to concerted deprotonation of the C-H bond during formation of the Pd-C bond.[5,21,26] Bringing the C-H bond to the correct geometry for a strong $\sigma_{(C\text{-}H)}$ or

Scheme 1. (a) General scheme of nickel catalysis of amides bearing 8-aminoquinoline (8AQ) directing group;[28-58] (b) ureas as substrates for α-(C-H) functionalization of nitrogenous compounds;[66,67] (c) *this work*: A study of nickel(II) mediated C(sp^3)-H activation of ureas as models for amides.

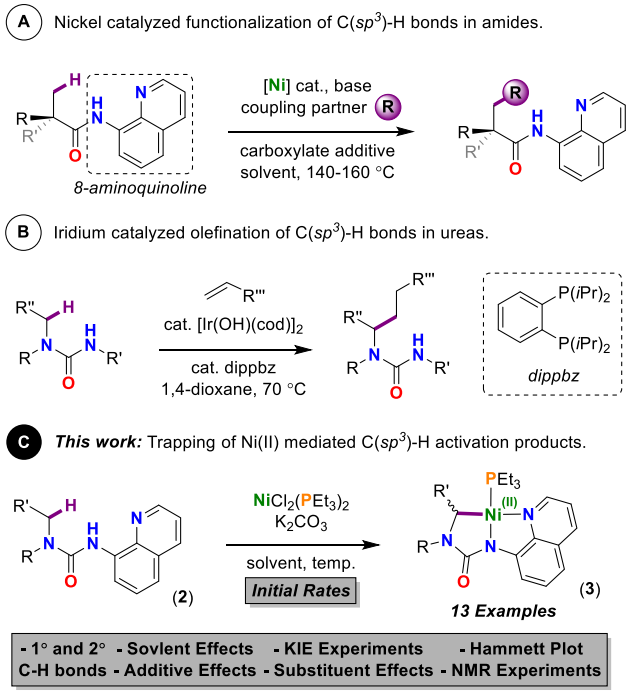

C-H agostic interaction plays an important part in polarizing the C-H bond. Carboxylate ligands on palladium have been shown computationally to further polarize the C-H bond by a hydrogen-bonding type interaction.[20,21,26] In the transition state, the carboxylate ligand is bound κ¹-O to palladium(II), and deprotonates the C-H bond to make a new Pd-C bond and a new O-H bond (see ESI, Figure S1). In principle, this process can be reversible, leading to protonation of the Pd-C bond.

Related work on CMD reactions with palladium suggests that a combination of bases, usually carbonate and carboxylate bases, increases the reaction rate and yield of catalytic

C-H functionalization methodologies. Elegant work by Rousseaux and Fagnou[5] suggests that for Pd(II) C(sp^3)-H activation of amides, hemi-labile carboxylates are integral to both lowering the CMD transition state energy, and facilitating dissociation of phosphine from palladium(II) intermediates. Other related work from Tsuji and Fujihara *et al.* showed that bulky carboxylate bases can effect facile Pd(II) C-H activation.[28]

Much less is known about the mechanism of Ni(II) mediated CMD reactions, despite the increasing focus on Ni-based catalysis. The most well-studied examples use Daugulis's 8-aminoquinoline (8AQ) directing group[29] (Scheme 1A, Scheme 2) to make new C-C,[30-52] C-N,[37,52,53] C-O,[40] C-S,[54-58] and even C-X[59-61] cross coupling products. This strategy has been applied to β-C(sp^2)-H[28-32,40,43,44,49,50,56-60] and β-C(sp^3)-H[30,31,49-57,59,32,63,36,40-44,46] bonds in amides. Calculations by Liu[64] and Sunoj[65] on the 8AQ-amide system suggest that the activation of secondary C(sp^3)-H bonds should be thermally accessible, however, the relative rates are projected to be lower than for primary substrates. This postulate is in contrast to the catalytic experimental observation that cyclic substrates with secondary C(sp^3)-H bonds are readily functionalized.[31,42,56] In some rare cases, substrates with acyclic secondary C(sp^3)-H bond functionalizations have been isolated.[36,53,59] The regioselectivity of primary C(sp^3)-H bonds is therefore due to the reductive elimination step, which is calculated to have higher barriers for secondary substrates.[64]

There are some significant limitations in the above methodologies for C(sp^3)-H bond functionalization: (i) substrates are generally limited to methyl, or cyclic alkyl derivatives; and (ii) each report uses different acid additives; there is no consensus on which carboxylates are optimal for C-H activation with Ni. Surprisingly, there are no experimental studies determining the factors which contribute to the efficacy of C(sp^3)-H activation at Ni(II). Moreover, no intermediates in the C(sp^3)-H functionalization of 8AQ-amides have been isolated. Therefore, to push the boundaries of C-H functionalization methodologies using earth abundant nickel catalysts, we must aim to understand the mechanism of the C-H activation step itself.

Recently, Nishimura *et al.* showed that secondary and tertiary ureas can be used as directing groups for iridium catalyzed C(sp^3)-H bond alkylation alpha to a nitrogen atom (Scheme 1b).[66,67] The authors suggest that iridium facilitates this reaction through an oxidative addition pathway. Although the reaction has been extended to indoline derivatives, the authors were not able to functionalize other substrates with secondary C(sp^3)-H bonds.[67]

Our group has long been interested in the chemistry of nickel and group 10 metals.[68-70] Inspired by the aforementioned Nishimura contribution, we imagined using 8-aminoquinoline-substituted tertiary ureas (Scheme 1C) as more reactive models for the 8AQ-amide catalysis pioneered by Daugulis. We hypothesized that by using ureas instead of amides, that the C-H bond should have a higher effective concentration at the metal center due to the conformation imposed by the π_N-π^*_{CO} bonding interaction. Additionally, we postulated that the increased acidity of C-H bonds alpha to a urea nitrogen atom would allow for trapping of the C-H activated intermediates by attenuating the basicity of the resulting Ni-C bond.

Scheme 2. Computationally derived mechanism of nickel(II) mediated C(sp^3)-H functionalization of 8AQ substituted amides.[62,63]

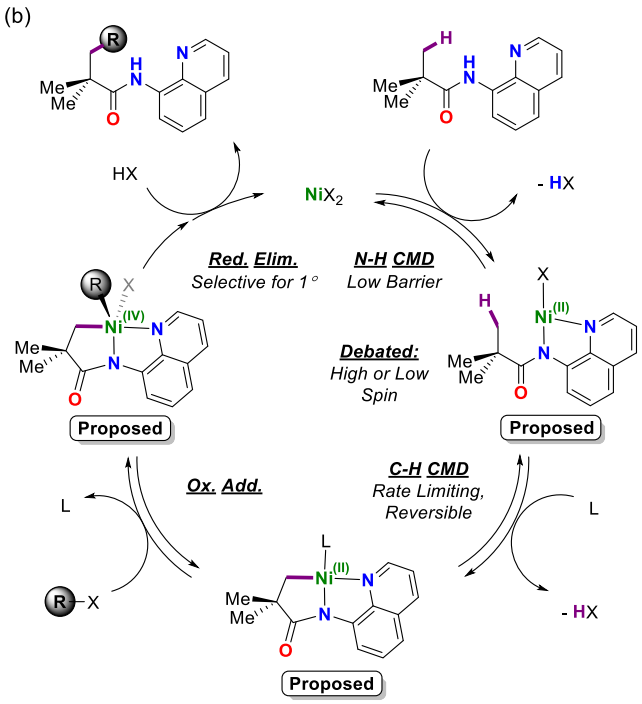

Herein, we show that by using simple nickel salts we can characterize, and in one case isolate, analogues of the previously proposed (*but not observed*) products of primary and secondary δ-C(sp^3)-H bond activation using 8AQ-substituted ureas as model substrates (Scheme 1C). Through a series of kinetic and mechanistic experiments we show that C-H bond activation is rate determining and reversible. We also probe the kinetic consequences of different solvents and additives. Additionally, a Hammett analysis supports a transition state with an electrophilic metal center, as expected for a CMD pathway.

Results and Discussion

(i) Reaction Discovery: We began by examining the C-H activation conditions of urea (**2a**); (Me)(Cy)N(CO)N(H)(quinolin-8-yl). After screening a variety of conditions, we found that heating (**2a**) in toluene in the presence of $NiCl_2(PEt_3)_2$ and K_2CO_3 led to the C(sp^3)-H activation product [(PEt_3)Ni(κ^3-*C,N,N*-($\underline{C}H_2$)N(Cy)(CO)N(($\underline{N}$)-quinolin-8-yl))] (**3a**) in moderate yield (Scheme 3). Unfortunately, long reaction times are required; however, we were able to scale this reaction up to gram scales of (**2a**) to isolate (**3a**) in reasonable quantities. We characterized (**3a**) by multinuclear and multidimensional NMR spectroscopy, X-ray diffraction (XRD), and elemental analysis.

Scheme 3. Synthesis of Ni(II) ureate (3a) by C(sp^3)-H activation of (2a).

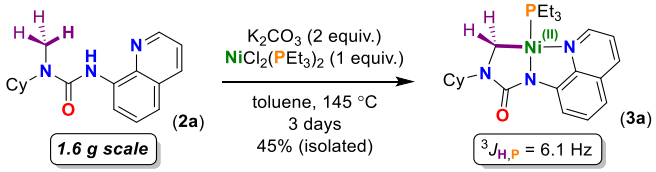

In the ^{1}H NMR spectrum of (**3a**) (d_8-toluene, 298 K), a characteristic doublet assigned to the cyclometalated Ni-CH_2 [δ 2.67] displays phosphorus coupling through the nickel center [$^3J_{H,P}$ = 6.1 Hz]. Coupling is not observed when phosphorus decoupling is employed. In the ^{31}P{^{1}H} NMR spectrum, the triethylphosphine signal is observed at [δ 18.9] as a sharp singlet. Additionally, in the ^{13}C NMR spectrum the urea (C=O) carbonyl resonance shifts downfield by over 8 ppm relative to (**2a**). Notably, in the presence of excess triethylphosphine the phosphine signal of (**3a**) broadens significantly and the (PEt$_3$)-Ni-CH_2 [$^3J_{H,P}$] coupling disappears in the ^{1}H NMR spectrum; this suggests rapid phosphine exchange at room temperature.

We isolated XRD quality single crystals of (**3a**) from toluene-hexamethyldisiloxane mixtures cooled to -35 °C. The solid-state molecular structure (Figure 1) reveals a square planar nickel center [$\Sigma\theta_{Ni}$ = 360.25(25)]. The carbon-nickel bond [C(1)-Ni(1) = 1.923(2)] is shorter than other Ni(II)-C(sp^3) bonds (see SI for list of other Ni(II)-C(sp^3) bond lengths),[71–74] likely due to the weak *trans*-influence of the quinoline nitrogen donor. Of note is the strain induced by the five-membered cyclometalated ring, where the angles made by (i) C(1)-N(1)-C(2) and (ii) N(1)-C(2)-N(2) are each reduced by five degrees compared to the solid-state structure of the proteoligand, (**2a**) [Δ(°) = (i) 5.1(2); (ii) 4.9(2)] (see ESI Figure S183 for solid-state structure of (**2a**)).

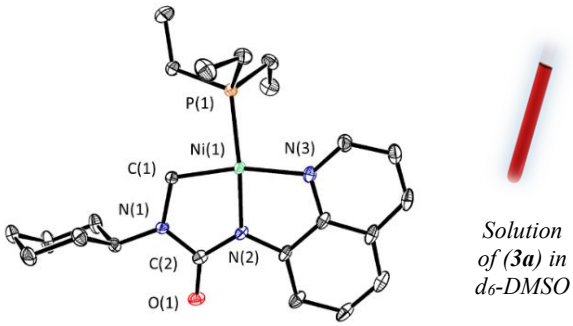

Figure 1. ORTEP depiction of the solid-state structure of complex (**3a**) (ellipsoids at 50% probability, hydrogens and solvent omitted). Selected bond lengths (Å) and angles (°): C1-Ni1 1.923(2), N2-Ni1 1.855(2), N3-Ni1 1,972(2), C2-O1 1.238(3), C1-Ni1-N3 166.5(1), N1-C1-Ni1 109.8(2).

(ii) Solvent Effects: Having characterized (**3a**), we sought to examine how solvent choice may affect the rate of C(sp^3)-H activation. Six solvents, in three distinct temperature regimes ranging from 70-145 °C were chosen (**Table 1**). Reactions in d_6-DMSO (DMSO = dimethyl sulfoxide) heated to 145 °C converted nearly half of (**2a**) to (**3a**) in five hours (entry 2). Moreover, we found that (**3a**) is produced appreciably even at 70 °C in DMSO (entry 5). Reactions in d_7-DMF (DMF = *N*,*N*-dimethylformamide) produced (**3a**) at comparable rates to d_6-DMSO reactions, however, in our hands reactions in d_7-DMF suffered from a lack of reproducibility (see SI).

Reactions prepared in chlorinated solvents d_2-tetrachloroethane (entry 1) and $CDCl_3$ (entry 7) resulted in decomposition to myriad paramagnetic products. In contrast, reactions in deuterated tetrahydrofuran (entry 6), and acetonitrile (entry 4) did produce (**3a**), but were sluggish compared to reactions in DMSO. Notably, reactions in acetonitrile have long induction periods.

These results show that coordinating polar aprotic solvents such as DMSO and DMF increase the rate of nickel mediated C(sp^3)-H activation of (**2a**). We reason that coordinating solvents may be beneficial for stabilizing an electropositive nickel center in the reaction coordinate, or the solvent may assist with substitution of triethylphosphine for the quinoline directing group.

Table 1. Effect of solvent on initial rates of formation of complex (3a)

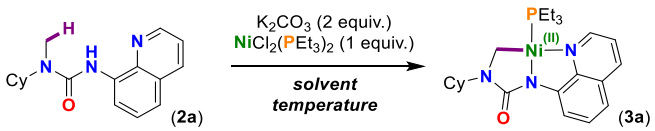

Entry	Solvent	Temperature (°C)	Rate[75] (M/min)
1	d_2-TCE	145	decomposition[a]
2	**d_6-DMSO**	**145**	**$t_{1/2}$ ~ 5 hours**
3	**d_6-DMSO**	**90**	**(3.3 ± 0.1) x 10^{-5}**
4	CD_3CN	90	complex (Fig. S105)
5	**d_6-DMSO**	**70**	**(6.9 ± 0.4) x 10^{-6}**
6	d_8-THF	70	negligible[b]
7	$CDCl_3$	70	decomposition[a]

[a]No product is observed, and myriad paramagnetic peaks are detected instead; [b]Over 36h, < 1% product formation by ^{1}H NMR spectroscopy.

(iii) Additive Effects: Using DMSO as our reaction solvent going forward, we screened different additives for their effects on the described C-H activation reaction (Scheme 4). In catalytic C-H functionalization methodologies, many research groups have found it advantageous to add bulky carboxylic acids or external bases. Thus, we screened a variety of carboxylate bases in the reaction of (2a) to (3a).[76]

We first conducted a series of reactions to establish baseline reactivity (Scheme 4). In the absence of carbonate base or additive, the reaction proceeds to ~2% yield after 150 minutes at 110 °C. The observation of product suggests that another component of the reaction (e.g. urea or phosphine) may facilitate C-H activation to some degree. It is likely that the acid which is produced is neutralized by substrate quinoline or PEt$_3$. When carbonate is present, the reaction proceeds slowly and levels off at low conversions. We postulate that this poor conversion is due to competitive substrate-phosphine binding as the reaction proceeds.

Addition of the bulky 1-admantyl carboxylic acid (AdCOOH) somewhat increased the rate of C-H activation compared to the control reactions without additives. However, the addition of the slightly smaller potassium pivalate (KOPiv) resulted in a more significant rate increase. Notably, these conditions at 110 °C in the presence of KOPiv exhibit reaction half lives of approximately thirty minutes at 110 °C; $t_{1/2}$ ~ 0.5 h (*c.f.* Table 1, no additive, $t_{1/2}$ ~ 5 h, 145 °C).

KOAc does not promote the reaction to the same degree as KOPiv, but the rate is faster than with AdCOOH. It appears then, that for the additives there is an optimal steric profile, where the reaction proceeds at the highest rate.

From a strictly electronic perspective, adding 1,3,5-trimethylbenzoic acid has an insignificant effect on the reaction rate; however, addition of 2,6-bis(trifluoromethyl)benzoic acid slightly decreases the rate of C-H activation (see ESI, Figure S107). The effect of carboxylate pK_a on CMD type reactions is complicated: in some cases more electron donating substituents and higher pK_a result in faster reactions,[77] while the opposite has also been observed.[78] More studies would be needed to understand the origin of the rate difference in this case. Regardless, our results show that carbonate and carboxylate salts work synergistically to increase the rate of C-H activation (see ESI, Figure S108).[5,79]

Scheme 4. Effect of additive on reaction rate and progress in formation of complex (3a) from (2a).[75]

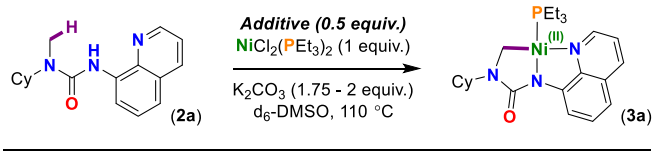

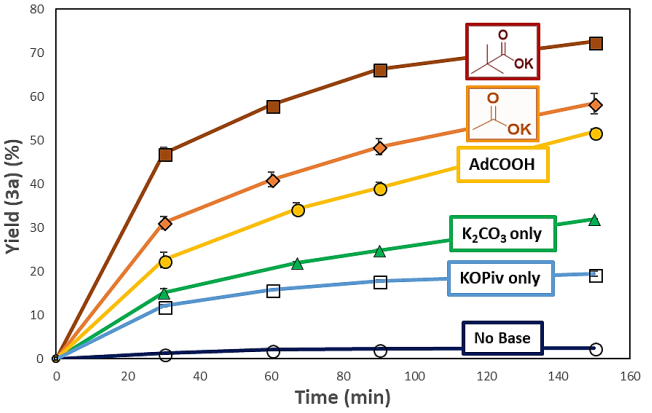

For (i) acid additives, 2.0 molar equivalents K_2CO_3 added, (ii) potassium salts, 1.75 molar equivalents K_2CO_3 added.[80] Legend: ○ No additive, or K_2CO_3, □ KOPiv added (No K_2CO_3), ▲ K_2CO_3 added (no additive); ● 1-adamantyl carboxylic acid additive; ◆ KOAc additive; ■ KOPiv additive.

(iv) Kinetic Isotope Effects (KIEs): Next, we wished to determine if C-H activation was the rate determining step in this reaction. Calculations done on the 8AQ-amide system vary in whether C-H activation is rate-determining in catalytic reactions,[64,65,81] although it has been shown that there can be difficulties when modelling additives.[82] To address this point, we synthesized the tri-deutero urea (**2a-d_3**) and the *N,N*-dimethyl substituted ureas (**2b**, **2b-d_3**) (Scheme 5). Only one methyl CH_3 signal is observed in the ^{1}H NMR spectra of (**2b**) and (**2b-d_3**), suggesting facile Me$_2$*N*-*C*(=O) bond rotation.

Using the optimized reaction conditions (solvent = d_6-DMSO, additive = KOPiv), we compared the independent initial rates of C-H activation for (**2a**) and (**2a-d_3**), which resulted in a strong primary intermolecular KIE (7.2 ± 0.4), suggesting that C(*sp*^{3})-H bond activation step is rate limiting. Our intramolecular KIE experiments with (**2b-d_3**) also confirm a large primary KIE for C(*sp*^{3})-H bond activation (6.8 ± 0.8). The magnitudes of our primary KIEs are similar to the intermolecular KIE for a Pd catalyzed reaction with amide C(*sp*^{3})-H activation substrates [c.f. KIE = 6.5].[5]

Scheme 5. Kinetic isotope effects for intra- and intermolecular C(*sp*^{3})-H bond activation in ureas.

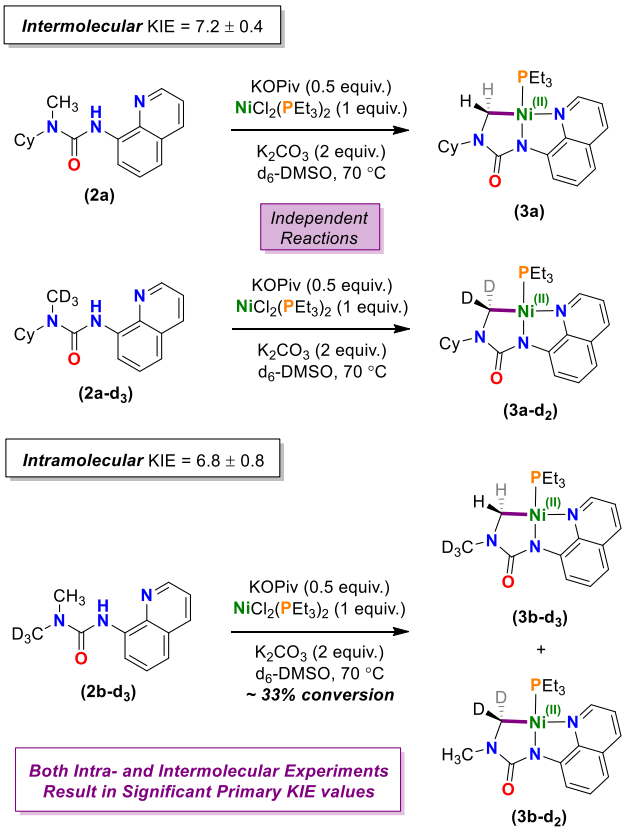

We next wished to probe whether C-H activation was reversible in our system. To explore the question of reversibility we started by adding different proton (H+) sources to isolated complex (**3a**) (Scheme 6). Upon heating at 70 °C in the presence of (**2a-d_3**) (Scheme 6a), we observed only trace amounts of (**2a**) from the protonation of the cyclometalated (**3a**), suggesting that the N-H in free urea (**2a-d_3**) can act as a proton source, but it is not significant. Interestingly, under standard reactions conditions with nickel and base, (**2a**) is not observed, suggesting that the protonation of (**3a**) is not from trace water. Adding the more acidic [HNMe$_2$Ph][B(C$_6$F$_5$)$_4$] leads to protonation of the Ni-C bond in (**3a**) to give (**2a**) even at room temperature (Scheme 6b). We next added the soluble carboxylic acid, AdCOOH, to probe whether carboxylate assisted CMD processes could, in principle, be reversible. No reaction is observed at room temperature, and heating to 70 °C for hours leads to only small amounts of protonation of (**3a**) to give (**2a**) (Scheme 6c). It appears then that C-H activation is *potentially* reversible under reaction conditions. However, only a small amount of free carboxylic acid would be produced; thus, we suggest that synthesis of (**3a**) is essentially irreversible under these conditions.

Scheme 6. Probing protonation of the Ni-C bond in (3a) with (a) deuterated urea (2a-d_3), (b) an anilinium salt, and (c) 1-adamantyl carboxylic acid.

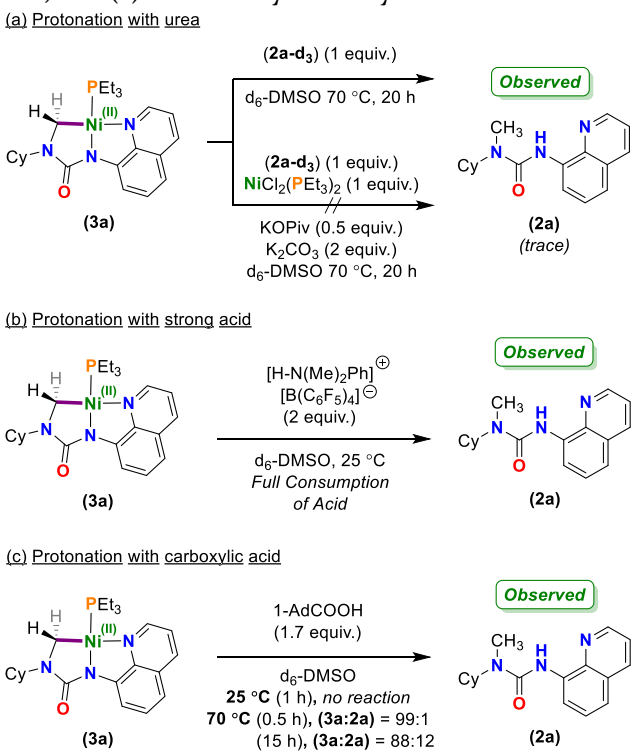

(v) Substrates with 2° δ-C(sp^3)-H Bonds: Our kinetic studies show that a range of other substrates (**2c,e-n**) are susceptible to C-H activation under these conditions (Scheme 7). Each of the resulting organometallic species (**3c,e-n**) was characterized by *in-situ* NMR spectroscopy and display similar spectroscopic characteristics to (**3a**). For instance, the products (**3c,e-n**) each show a singlet in the $^{31}P\{^1H\}$ NMR spectrum between [δ 15.7-21.3] corresponding to a single PEt_3. Like (**3a**), the ^1H-^{13}C HMBC NMR spectra show a shift [Δ(ppm) > 5] of the urea carbonyl (C=O) resonance downfield upon cyclometalation.

Ethyl-substituted (**2c**) undergoes C(sp^3)-H activation, with a k_{rel} ~ 2.4 at 90 °C (k_{rel} of (**2a**) was arbitrarily set to 100 for ease of comparison). *Via* Eyring analysis, we estimate the relative barriers to C-H activation for (**2a**) versus (**2c**) to be approximately [$\Delta\Delta G^{\neq}_{exp}$ = 2.7 kcal/mol]. In a recent computational report by Omar and Lui,[64] the authors compared the C-H activation barriers between a methyl and ethyl group for nickel mediated C(sp^3)-H activation of 8AQ-amides [$\Delta\Delta G^{\neq}_{calc}$ = 2.8 kcal/mol]. Thus, our results agree nicely with calculations done on the 8AQ-amide chemistry. Substrate (**2d**) bearing a tertiary isopropyl group is not amenable to C-H activation under these conditions, likely due to steric limitations.

Surprisingly, reactions with benzyl substrates (**2e-j**) display reaction rates that are comparable to (**2a**) at 70 °C. The rate is highest for electron rich aryl rings adjacent to the reactive C-H bond. A Hammett analysis shows a linear correlation for substrates (**2e-j**) (Scheme 8, R^2 = 0.96). Curiously, the effect of electronics on CMD type reactions can vary depending on the system and reaction conditions. In some cases, electron withdrawing substituents can result in increased rates of C-H activation,[23,83] while in other cases electron donating substituents result in higher rates.[84-86] The negative ρ value (-0.39), although small in magnitude, is consistent with an electrophilic C-H activation transition state (*c.f.* KIEs) that has a build-up of positive charge. We propose that increased C-H electron density leads to stronger C-H agostic interactions, increasing the rate of C-H activation.

Cyclic substrates derived from saturated *N*-heterocycles (**2l-n**) also react at comparable rates to (**2c**). The smaller azetidine derivative (**2k**) does not form significant quantities of product (**3k**) under these conditions. Our rate data suggest that larger rings react faster than smaller rings. We attribute this effect to a decreased distance of the δ-C(sp^3)-H bond from the metal center, increasing the C-H effective concentration at the metal center.

Scheme 7. Relative reaction rates for C-H activation of ureas (2a,c-n) to nickel products (3a,c-n).[75]

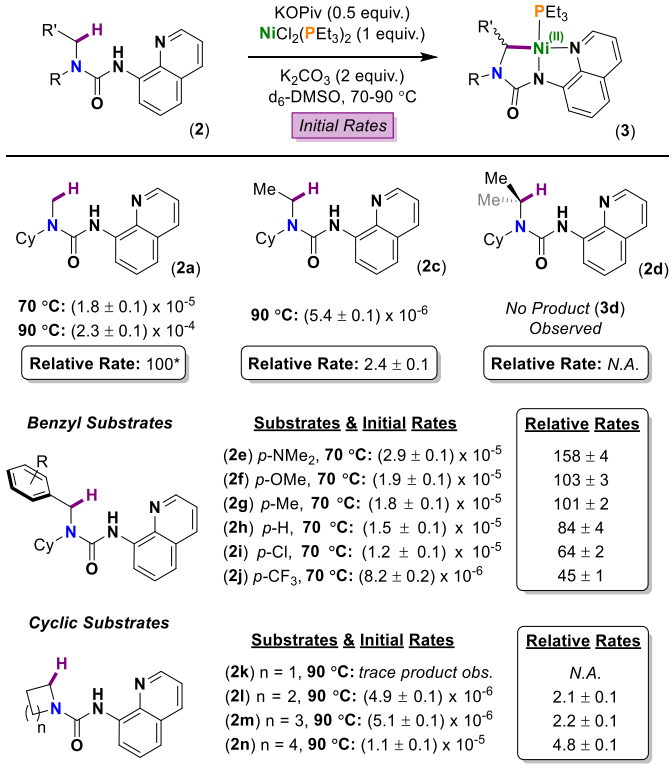

Rate units in M/min. *Rate of (**2a**) arbitrarily set to 100.

(iv) Investigating Role of KOPiv: Encouraged by results with ureas (**2a-c,e-n**), and the increased reaction rates with carboxylate additives, we began further mechanistic studies to determine the origins of increased reaction rates when pivalate is added to nickel. When KOPiv is added to $NiCl_2(PEt_3)_2$ (Scheme 9a), we observe new paramagnetic peaks in the ^1H NMR spectrum (d_6-DMSO, 298 K). Adding two equivalents of PEt_3 to a known Ni(II) dimer, $[(NEt_3)Ni(\mu\text{-}OPiv)_2]_2$ gave us the same paramagnetic resonances in the ^1H NMR spectrum. We reasoned the pivalate ions could promote dimerization of two nickel(II) centers, as is common in palladium(II) chemistry.[13,87] Upon crystallization, we isolated paddlewheel complex (**4**), $[(PEt_3)Ni(\mu\text{-}OPiv)_2]_2$, as large green-yellow iridescent crystals. We characterized (**4**) by ^1H NMR spectroscopy, elemental analysis, the Evans method, and single crystal XRD.

Scheme 8. Hammett Plot showing rates of δ-C(*sp*³)-H activation of *p*-benzyl substituted ureas (2e-j).[75]

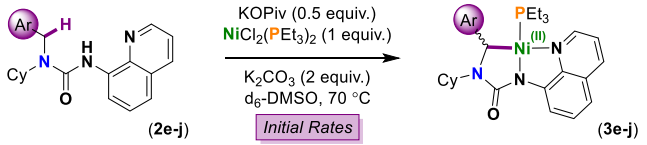

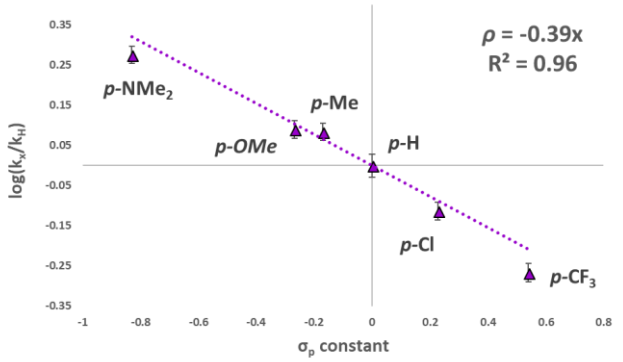

Scheme 9. (a) Synthesis of (4) by two methods, and (b) ORTEP depiction of the solid-state structure of complex (4) (ellipsoids at 50% probability, hydrogens omitted). Selected bond lengths (Å) and angles (°): Ni-Ni 2.5875(3), O1-Ni1-P1 96.60(3).

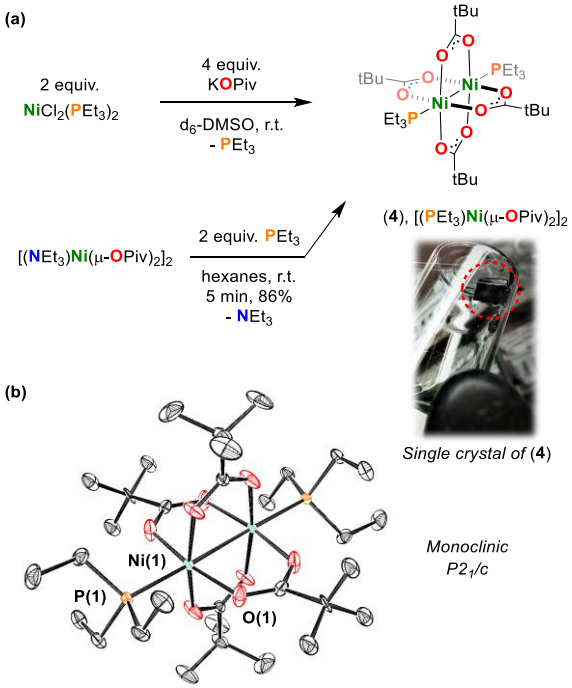

In the solid-state, complex (**4**) exhibits a paddlewheel type structure, where the nickel centers are bridged by four pivalate ions and capped by triethylphosphine ligands. Complex (**4**) exhibits a shortened Ni-Ni distance [Ni-Ni; 2.5875(3) Å] relative to the related triethylamine derivative [c.f. Ni-Ni; 2.728(2)].[88] Based on these results, we reasoned that pivalate-induced dimerization may be integral to increasing the rate of phosphine dissociation from Ni(II), much like in the case of Pd(II).[5] Unfortunately, the poor solubility of (**4**) in d_6-DMSO prevents us from comparing the rates of C-H activation with (**2a**). Moreover, if solutions of $NiCl_2(PEt_3)_2$ and KOPiv are left overnight (d_6-DMSO, 298 K), green solids crash out of the reaction, suggesting formation of complex (**4**) in-situ.

We then examined the role of pivalate in the presence of ureas, pre-(C-H) activation. Upon addition of (**2a**) to solutions of $NiCl_2(PEt_3)_2$ and KOPiv (Scheme 10, reaction **II**), new paramagnetic peaks are observed in the ^{1}H NMR spectrum. These peaks are also observed upon the addition of (**2a**) to complex (**4**) (reaction **IV**), further supporting the formation of (**4**) upon mixing $NiCl_2(PEt_3)_2$ and KOPiv. These same paramagnetic peaks are observed when (**2a**) is added to $[(NEt_3)Ni(\mu\text{-}OPiv)_2]_2$ (reaction **VI**), suggesting that phosphine is not incorporated in the paramagnetic complex.

Scheme 10. ^{1}H paramagnetic NMR spectra for different reactions; outlined in the general reaction scheme, and a table showing the reaction contents for reactions (I-VI, d_6-DMSO, 400 MHz, 298 K).

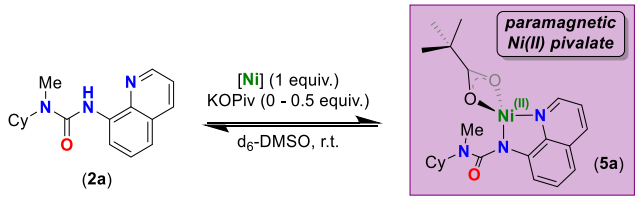

ESI MS m/z = 441.1
calc. (5a); 441.2

Reaction	[Ni] complex	Urea	KOPiv
(I)	$NiCl_2(PEt_3)_2$	-	0.5 equiv.
(II)	$NiCl_2(PEt_3)_2$	(**2a**)	0.5 equiv.
(III)	(**4**)	-	-
(IV)	(**4**)	(**2a**)	-
(V)	$[(NEt_3)Ni(\mu\text{-}OPiv)_2]_2$	-	-
(VI)	$[(NEt_3)Ni(\mu\text{-}OPiv)_2]_2$	(**2a**)	-

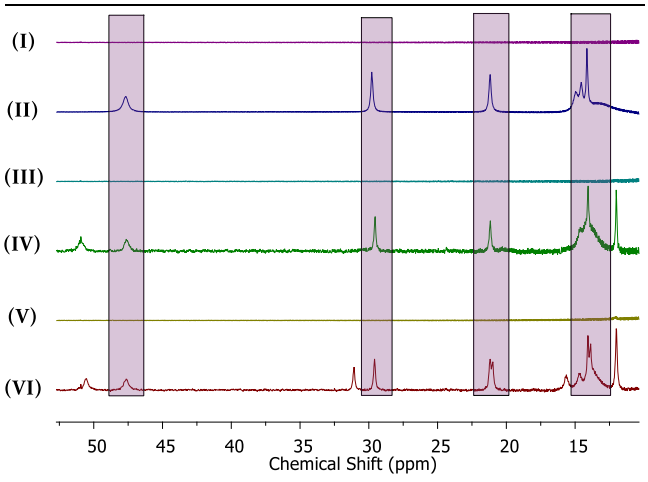

Based on the above stoichiometric results, we propose two possible paramagnetic nickel structures: (i) a simple Lewis base adduct of the urea quinoline *via* phosphine displacement, or (ii) the N-H activated product (**5a**). We tested this hypothesis by synthesizing compound (**2a-Me**), where the N-H is replaced by a N-CH_3 group. This substitution should not affect the Lewis base adduct but should stop the formation of an X-type Ni-N bond as in (**5a**). Upon

addition of (**2a-Me**) to complex (**4**) (Scheme 11), we observed no paramagnetic resonances after days of stirring, suggesting that the paramagnetic resonances belong to (**5a**) and not the Lewis base adduct of the quinoline.

The above stoichiometric NMR scale reactions suggest that the Ni(II) ureate pre-(C-H) activation is a high spin complex, presumably tetrahedral or octahedral. At this time, we favor the idea that (**5a**) is a monomer, although we cannot rule out dimer formation in solution. Electrospray-ionization mass spectrometry suggests the (**5a**) is present in solution (see SI, Figure S133), although we have not quantified the concentration of this product.

Scheme 11. Probing reactivity of (2a-Me) with nickel complex (4).

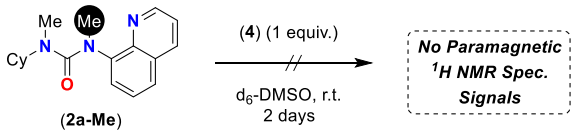

In the ^{1}H NMR spectra of reactions **II**, **IV**, and **VI** (Scheme 10) unbound (**2a**) is visible, but is significantly broadened. We propose an equilibrium between (**2a**) and (**5a**), among other probable nickel products. Additionally, the formation of (**5a**) at room temperature suggests that N-H cleavage is facile. This has been previously proposed in computational studies of the analogous catalytic system with 8AQ substituted amides.[64]

Finally, we wished to see if cyclometalated (**3a**) would undergo further reactivity to functionalize the C-Ni bond. We chose a variety of coupling partners to show the potential of C(*sp*^{3})-H functionalizations of ureas (Scheme 12). Addition of an α-bromoketone resulted in the formation of a new C-C bond to produce (**2o**) in good yields. Likewise, we were also able to form new C-C bonds by additions of an aryl iodonium salt or PhI to produce (**2p**) and (**2h**) respectively. Insertion reactions of CO were also productive, resulting in the formation of new C-C and C-N bonds in the cyclized urea (**2q**), which we prepared independently (See SI). These results suggest (**3a**) is a relevant intermediate in nickel mediated C(sp^3)-H functionalizations.

Scheme 12. Reactivity of complex (3a) with a variety of coupling partners. For reaction conditions, see SI. (^{1}H NMR spectroscopic yields, Q = quinolin-8-yl)

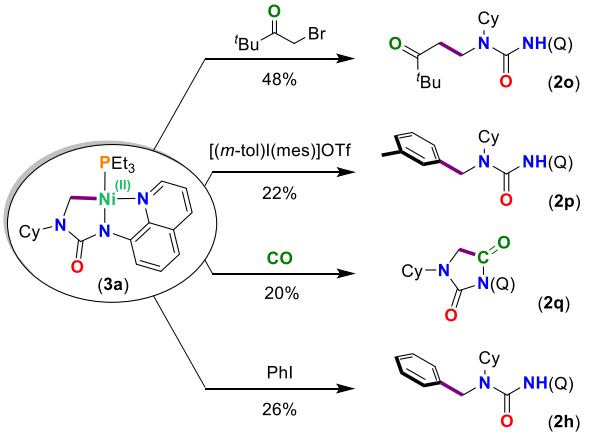

Based on the kinetic and mechanistic data we present in this manuscript, we suggest the following mechanism for C-H activation (Scheme 13). When KOPiv is added to $NiCl_2(PEt_3)_2$, a salt metathesis reaction produces (**4**). NMR scale reactions (Schemes 9-11) suggest that pivalate is important for facile N-H activation, and dissociation of phosphine. Upon addition of urea (**2**), complex (**5**) is produced, which was shown by paramagnetic ^{1}H NMR studies (Schemes 10, 11) and supported by mass spectrometry. KIE experiments suggest then that the C-H activation step is rate limiting (Scheme 5), and protonation studies suggest reversibility is probable (Scheme 6). We isolated the C-H activation product (**3a**, Scheme 3) and showed that different additives have a profound effect on the rate of product formation of (**3a**) (Table 1). Namely, carboxylate additives ($RCOO^-$) show a steric dependence on the carboxylate R-group. We also showed that substrates (**2c,e-n**) with secondary C(*sp*^{3})-H bonds may be C-H activated (Scheme 7), and these substrates are produced at a higher rate for more electron rich derivatives (Scheme 8). Finally, we show that (**3a**) reacts with myriad electrophiles to afford C-C and C-N coupling products, suggesting that (**3a**) is a relevant intermediate in the nickel catalyzed C(*sp*^{3})-H functionalization of 8AQ-amides.

Scheme 13. Proposed mechanism for the Ni(II) mediated δ-C(*sp*^{3})-H activation of substituted ureas.

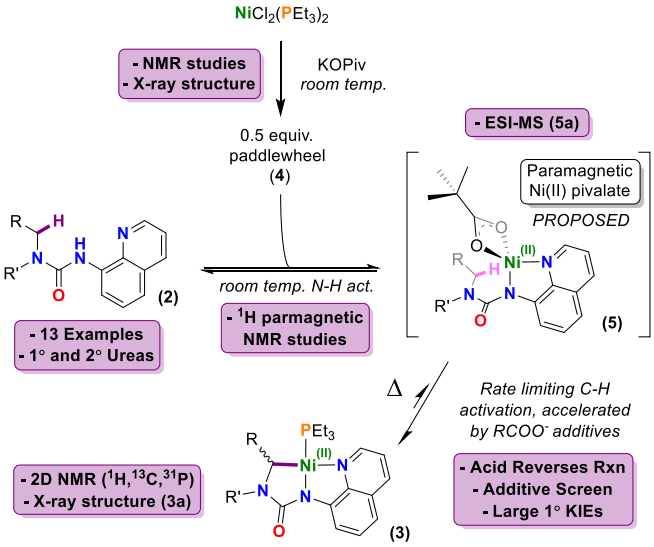

Conclusions

We showed in this work that using ureas as model substrates, we can investigate the elementary steps of C(*sp*^{3})-H activation at nickel(II) centers. By using the 8AQ directing group, we measured the rates of C-H activation for primary and secondary C-H bonds and showed that C-H activation is rate limiting prior to functionalization. Additionally, we investigated the role of carboxylate additives, showing that they increase the rate of phosphine dissociation, N-H activation, and C-H activation.

Current work in our group is focused on probing kinetic consequences of the directing group, including electronic properties of the 8-aminoquinoline moiety. We anticipate this work will facilitate the discovery of important trends

in nickel-catalyzed C-H activation, leading to the development of more efficient methodologies with broader scope. In addition, we have been focused on applying our discovery of nickel mediated urea C(sp^3)-H bond activation to catalytic methodologies, which we anticipate may be used to advantage the alpha functionalization of amide-directed amines.

ASSOCIATED CONTENT

(Supporting Information)

See ESI for NMR spectra for all compounds as well as crystallographic data for (**2a**), (**3a**), and (**4**)**.** Kinetic data plots are also included. The supporting information is available free of charge on the ACS Publications website at DOI: XXXXX. CCDC 1853556-1853558 contain the supplementary crystallographic data for this paper. These data can be obtained free of charge from the Cambridge Crystallographic Data Centre via www.ccdc.cam.ac.uk/data_request/cif.

AUTHOR INFORMATION

Corresponding Author

*E-mail for L.L.S.: lschafer@chem.ubc.ca.
*E-mail for J.A.L.: jenlove@chem.ubc.ca.

Notes:

The authors declare no competing financial interests.

ACKNOWLEDGMENT

The authors thank: NSERC (Discovery, CREATE, and Instrumentation Grants to JAL and LLS), The University of British Columbia (4YF, Laird to DDB) and the government of Canada (NSERC PGSD to DDB). This work was undertaken, in part, thanks to funding from the Canada Research Chairs program (LLS).

REFERENCES

((1) Waltz, K. M.; Hartwig, J. F. *Science* **1997**, *277* (5323), 211–213.
(2) Wax, M. J.; Stryker, J. M.; Buchanan, J. M.; Kovac, C. A.; Bergman, R. G. *J. Am. Chem. Soc.* **1984**, *106* (4), 1121–1122.
(3) Janowicz, A. H.; Periana, R. A.; Buchanan, J. M.; Kovac, C. A.; Stryker, J. M.; Wax, M. J.; Bergman, R. G. *Pure Appl. Chem.* **1984**, *56* (1), 13–23.
(4) Chen, H.; Schlecht, S.; Semple, T. C.; Hartwig, J. F. *Science* **2000**, *287* (5460), 1995–1997.
(5) Rousseaux, S.; Gorelsky, S. I.; Chung, B. K. . W.; Fagnou, K. *J. Am. Chem. Soc.* **2010**, *132* (31), 10692–10705.
(6) Zhang, Y.; Shi, B.; Yu, J. *J. Am. Chem. Soc.* **2009**, *131* (14), 5072–5074.
(7) Shaw, M. H.; Shurtleff, V. W.; Terrett, J. A.; Cuthbertson, J. D.; MacMillan, D. W. C. *Science* **2016**, *352* (6291), 1304–1308.
(8) Joe, C. L.; Doyle, A. G. *Angew. Chem. Int. Ed.* **2016**, *55* (12), 4040–4043.
(9) Cuthbertson, J. D.; MacMillan, D. W. C. *Nature* **2015**, *519* (7541), 74–77.
(10) McNally, A.; Prier, C. K.; MacMillan, D. W. C. *Science* **2011**, *334*, 1114–1117.
(11) Zuo, Z.; Ahneman, D. T.; Chu, L.; Terrett, J. A.; Doyle, A. G.; MacMillan, D. W. C. *Science* **2014**, *345* (6195), 437–440.
(12) Desai, L. V; Stowers, K. J.; Sanford, M. S. *J. Am. Chem. Soc.* **2008**, 13285–13293.
(13) Lyons, T. W.; Sanford, M. S. *Chem. Rev.* **2010**, *110* (2), 1147–1169.
(14) Rouquet, G.; Chatani, N. *Angew. Chem. Int. Ed.* **2013**, *52* (45), 11726–11743.
(15) Campeau, L.-C.; Schipper, D. J.; Fagnou, K. *J. Am. Chem. Soc.* **2008**, *130* (11), 3266–3267.
(16) Wang, X.-C.; Gong, W.; Fang, L.-Z.; Zhu, R.-Y.; Li, S.; Engle, K. M.; Yu, J.-Q. *Nature* **2015**, *519* (7543), 334–338.
(17) Lu, Q.; Glorius, F. *Angew. Chem. Int. Ed.* **2017**, *56* (1), 49–51.
(18) Yi, H.; Zhang, G.; Wang, H.; Huang, Z.; Wang, J.; Singh, A. K.; Lei, A. *Chem. Rev.* **2017**, *117* (13), 9016–9085.
(19) Waterman, R. *Organometallics* **2013**, *32* (24), 7249–7263.
(20) Boutadla, Y.; Davies, D. L.; Macgregor, S. A.; Poblador-Bahamonde, A. I. *Dalton Trans.* **2009**, No. 30, 5820–5831.
(21) Gorelsky, S. I.; Lapointe, D.; Fagnou, K. *J. Org. Chem.* **2012**, *77* (1), 658–668.
(22) Lapointe, D.; Fagnou, K. *Chem. Lett.* **2010**, *39* (11), 1118–1126.
(23) Gorelsky, S. I.; Lapointe, D.; Fagnou, K. *J. Am. Chem. Soc.* **2008**, *130* (33), 10848–10849.
(24) We Will Refer to This Heteroatom Assisted C-H Activation Mechanism as CMD for the Duration of This Manuscript. We Do so for Ease of Discussion, and We Acknowledge Other Equally Valid Descriptions Such as Ambiphilic Metal Ligand Activation.
(25) Guihaumé, J.; Halbert, S.; Eisenstein, O.; Perutz, R. N. *Organometallics* **2012**, *31* (4), 1300–1314.
(26) Davies, D. L.; Donald, S. M. A.; Macgregor, S. A. *J. Am. Chem. Soc.* **2005**, *127* (40), 13754–13755.
(27) Lyons, T.; Sanford, M. *Chem. Rev.* **2010**, 1147–1169.
(28) Tanji, Y.; Mitsutake, N.; Fujihara, T.; Tsuji, Y. *Angew. Chem. Int. Ed.* **2018**, 1–5.
(29) Zaitsev, V. G.; Shabashov, D.; Daugulis, O. *J. Am. Chem. Soc.* **2005**, *127* (38), 13154–13155.
(30) Wu, X.; Zhao, Y.; Ge, H. *J. Am. Chem. Soc.* **2014**, *136* (5), 1789–1792.
(31) Iyanaga, M.; Aihara, Y.; Chatani, N. *J. Org. Chem.* **2014**, *79* (24), 11933–11939.
(32) Aihara, Y.; Chatani, N. *J. Am. Chem. Soc.* **2014**, *136* (3), 898–901.
(33) Li, M.; Dong, J.; Huang, X.; Li, K.; Wu, Q.; Song, F.; You, J. *Chem. Commun.* **2014**, *50* (30), 3944–3946.
(34) Aihara, Y.; Tobisu, M.; Fukumoto, Y.; Chatani, N. *J. Am. Chem. Soc.* **2014**, *136* (44), 15509–15512.
(35) Aihara, Y.; Wuelbern, J.; Chatani, N. *Bull. Chem. Soc. Jpn.* **2015**, *88* (3), 438–446.
(36) Liu, Y.-J.; Zhang, Z.-Z.; Yan, S.-Y.; Liu, Y.-H.; Shi, B.-F. *Chem. Commun.* **2015**, *51* (37), 7899–7902.
(37) Wang, X.; Zhu, L.; Chen, S.; Xu, X.; Au, C. T.; Qiu, R. *Org. Lett.* **2015**, *17* (21), 5228–5231.
(38) Maity, S.; Agasti, S.; Earsad, A. M.; Hazra, A.; Maiti, D. *Chem. Eur. J.* **2015**, *21* (32), 11320–11324.
(39) Wu, X.; Zhao, Y.; Ge, H. *J. Am. Chem. Soc.* **2015**, *137* (15), 4924–4927.
(40) Li, M.; Yang, Y.; Zhou, D.; Wan, D.; You, J. *Org. Lett.* **2015**, *17* (10), 2546–2549.
(41) Misal Castro, L. C.; Obata, A.; Aihara, Y.; Chatani, N. *Chem. Eur. J.* **2016**, *22* (4), 1362–1367.
(42) Cheng, Y.; Wu, Y.; Tan, G.; You, J. *Angew. Chem. Int. Ed.* **2016**, *55* (40), 12275–12279.
(43) He, Z.; Huang, Y. *ACS Catal.* **2016**, *6* (11), 7814–7823.
(44) Uemura, T.; Yamaguchi, M.; Chatani, N. *Angew. Chem. Int. Ed.* **2016**, *55* (9), 3162–3165.
(45) Obata, A.; Ano, Y.; Chatani, N. *Chem. Sci.* **2017**, *8* (9), 6650–6655.
(46) Honeycutt, A. P.; Hoover, J. M. *ACS Catal.* **2017**, *7* (7), 4597–4601.
(47) Sasagawa, A.; Yamaguchi, M.; Ano, Y.; Chatani, N. *Isr. J. Chem.* **2017**, *57* (10), 964–967.
(48) Luo, F. X.; Cao, Z. C.; Zhao, H. W.; Wang, D.; Zhang, Y. F.; Xu, X.; Shi, Z. J. *Organometallics* **2017**, *36* (1), 18–21.
(49) Wang, X.; Xie, P.; Qiu, R.; Zhu, L.; Liu, T.; Li, Y.; Iwasaki, T.; Au, C. T.; Xu, X.; Xia, Y.; et al. *Chem. Commun.* **2017**, *53* (59), 8316–8319.
(50) Tan, G.; Zhang, L.; Liao, X.; Shi, Y.; Wu, Y.; Yang, Y.; You, J. *Org. Lett.* **2017**, *19* (18), 4830–4833.
(51) Lin, C.; Chen, Z.; Liu, Z.; Zhang, Y. N *Org. Lett.* **2017**, *19* (4), 850–853.
(52) Li, J.; Zheng, Z.; Xiao, T.; Xu, P. F.; Wei, H. *Asian J. Org. Chem.* **2018**, *7* (1), 133–136.
(53) Wu, X.; Zhao, Y.; Ge, H. *Chem. Eur. J.* **2014**, *20* (31), 9530–9533.
(54) Wang, X.; Qiu, R.; Yan, C.; Reddy, V. P.; Zhu, L.; Xu, X.; Yin, S.-F. *Org. Lett.* **2015**, *17* (8), 1970–1973.

(55) Ye, X.; Petersen, J. L.; Shi, X. *Chem. Commun.* **2015**, *51* (37), 7863–7866.

(56) Lin, C.; Yu, W.; Yao, J.; Wang, B.; Liu, Z.; Zhang, Y. *Org. Lett.* **2015**, *17* (5), 1340–1343.

(57) Yan, S.-Y.; Liu, Y.-J.; Liu, B.; Liu, Y.-H.; Zhang, Z.-Z.; Shi, B.-F. *Chem. Commun.* **2015**, *51* (34), 7341–7344.

(58) Yokota, A.; Chatani, N. *Chem. Lett.* **2015**, *44* (7), 902–904.

(59) Aihara, Y.; Chatani, N. *ACS Catal.* **2016**, *6* (7), 4323–4329.

(60) Khan, B.; Kant, R.; Koley, D. *Adv. Synth. Catal.* **2016**, *358* (14), 2352–2358.

(61) Iwasaki, M.; Miki, N.; Tsuchiya, Y.; Nakajima, K.; Nishihara, Y. *Org. Lett.* **2017**, *19* (5), 1092–1095.

(62) Yokota, A.; Aihara, Y.; Chatani, N. *J. Org. Chem.* **2014**, *79* (24), 11922–11932.

(63) Wang, C.; Zhang, L.; You, J. *Org. Lett.* **2017**, *19* (7), 1690–1693.

(64) Omer, H. M.; Liu, P. *J. Am. Chem. Soc.* **2017**, *139* (29), 9909–9920.

(65) Singh, S.; K, S.; Sunoj, R. B. *J. Org. Chem.* **2017**, *82* (18), 9619–9626.

(66) Yamauchi, D.; Nishimura, T.; Yorimitsu, H. *Angew. Chem. Int. Ed.* **2017**, *56* (25), 7200–7204.

(67) Nakamura, I.; Yamauchi, D.; Nishimura, T. *Asian J. Org. Chem.* **2018**, No. Table 2, 1–5.

(68) Desnoyer, A. N.; Bowes, E. G.; Patrick, B. O.; Love, J. A. *J. Am. Chem. Soc.* **2015**, *137* (40), 12748–12751.

(69) Beattie, D. D.; Bowes, E. G.; Drover, M. W.; Love, J. A.; Schafer, L. L. *Angew. Chem. Int. Ed.* **2016**, *55* (42), 13290–13295.

(70) LaBerge, N. A.; Love, J. A. *Eur. J. Org. Chem.* **2015**, *2015* (25), 5546–5553.

(71) Gutsulyak, D. V.; Piers, W. E.; Borau-Garcia, J.; Parvez, M. *J. Am. Chem. Soc.* **2013**, *135* (32), 11776–11779.

(72) LaPierre, E. A.; Piers, W. E.; Spasyuk, D. M.; Bi, D. W. *Chem. Commun.* **2016**, *52* (7), 1361–1364.

(73) Kessler, J. A.; Iluc, V. M. *Dalton Trans.* **2017**, *46* (36), 12125–12131.

(74) Schultz, M.; Eisenträger, F.; Regius, C.; Rominger, F.; Hanno-Igels, P.; Jakob, P.; Gruber, I.; Hofmann, P. *Organometallics* **2012**, *31* (1), 207–224.

(75) NMR Yields (1H): Average of 2-3 Runs, 1,3,5-Trimethoxybenzene Was Used as an Internal Standard.

(76) The Central Results Are Shown in Scheme 4: For a Detailed List of Reaction Additives Tested, See SI.

(77) Cannon, J. S.; Zou, L.; Liu, P.; Lan, Y.; O'Leary, D. J.; Houk, K. N.; Grubbs, R. H. *J. Am. Chem. Soc.* **2014**, *136* (18), 6733–6743.

(78) Boutadla, Y.; Davies, D. L.; Macgregor, S. A.; Poblador-Bahamonde, A. I. *Dalton Trans.* **2009**, 30, 5887.

(79) Xu, H.; Muto, K.; Yamaguchi, J.; Zhao, C.; Itami, K.; Musaev, D. G. *J. Am. Chem. Soc.* **2014**, *136* (42), 14834–14844.

(80) A Further 0.25 Equivalents of K2CO3 Are Added for the Reaction with Addition of AdCOOH. This Ensures Similar Base Profiles to Reactions with Potassium Carboxylate Additives.

(81) Haines, B. E.; Yu, J.-Q.; Musaev, D. G. *Chem. Sci.* **2018**, *9* (5), 1144–1154.

(82) Davies, D. L.; Macgregor, S. A.; McMullin, C. L. *Chem. Rev.* **2017**, *117* (13), 8649–8709.

(83) Sun, H. Y.; Gorelsky, S. I.; Stuart, D. R.; Campeau, L. C.; Fagnou, K. *J. Org. Chem.* **2010**, *75* (23), 8180–8189.

(84) Stephens, D. E.; Lakey-Beitia, J.; Atesin, A. C.; Ateşin, T. A.; Chavez, G.; Arman, H. D.; Larionov, O. V. *ACS Catal.* **2015**, *5* (1), 167–175.

(85) Alharis, R. A. Electronic Effect on C-H Activation at Half Sandwich Complexes of Ir, Rh, and Ru. Doctor of Philosophy, University of Leicester, Leicester, United Kingdom, February 2018.

(86) Ryabov, A. D.; Sakodinskaya, I. K.; Yatsimirsky, A. K. *J. Chem. Soc. Dalt. Trans.* **1985**, No. 12, 2629.

(87) Powers, I. G.; Uyeda, C. *ACS Catal.* **2017**, *7* (2), 936–958.

(88) Eremenko, I. L.; Nefedov, S. E.; Sidorov, A. A.; Golubnichaya, M. A.; Danilov, P. V; Ikorskii, V. N.; Shvedenkov, Y. G.; Novotortsev, V. M.; Moiseev, I. I. *Inorg. Chem.* **1999**, *38* (17), 3764–3773.

Insert Table of Contents artwork here